

COMPUTATIONAL DESIGN AND PERFORMANCE PREDICTION OF CREEP-RESISTANT FERRITIC SUPERALLOYS

Peter K. Liaw¹, David C. Dunand², Gautam Ghosh², Michael Rawlings², Gian Song¹, Zhiqian Sun¹, Shao-Yu Wang¹, Morris E. Fine², Yanfei Gao¹, Gongyao Wang¹, Lin Li¹, Zhenke Teng¹, Shenyang Huang¹, Xiandong Xu⁵, Christian H. Liebscher³, Bjørn Clausen⁴, Jonathan Poplawsky⁶, Donovan N. Leonard⁶, Mark D. Asta³, Chain T. Liu⁷, Mingwei Chen⁵.

¹Department of Materials Science and Engineering, The University of Tennessee, Knoxville

²Department of Materials Science and Engineering, Northwestern University

³Department of Materials Science and Engineering, University of California, Berkeley

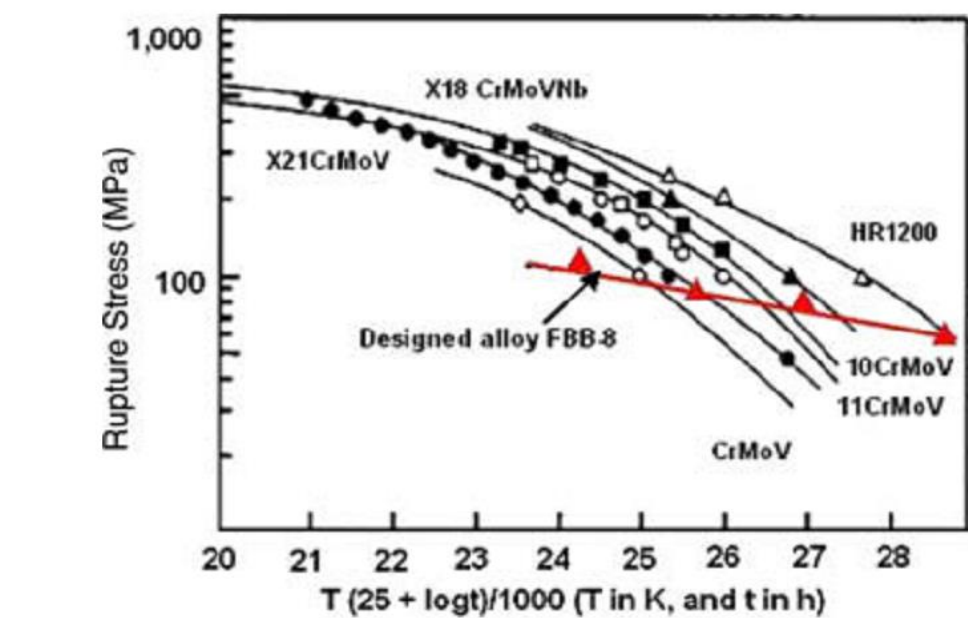
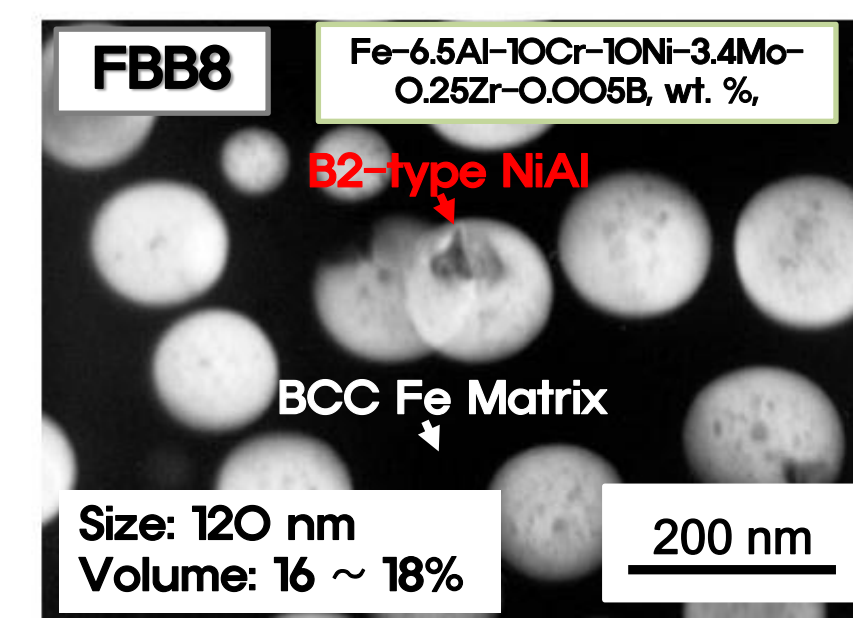
⁴Lujan Center, Los Alamos National Laboratory, Los Alamos

⁵WPI Advanced Institute for Materials Research, Tohoku University

⁶Center for Nano-phase Materials Sciences, Oak Ridge National Laboratory

⁷Center for Advanced Structural Materials, MBE Department, City University of Hong Kong, Kowloon, Hong Kong

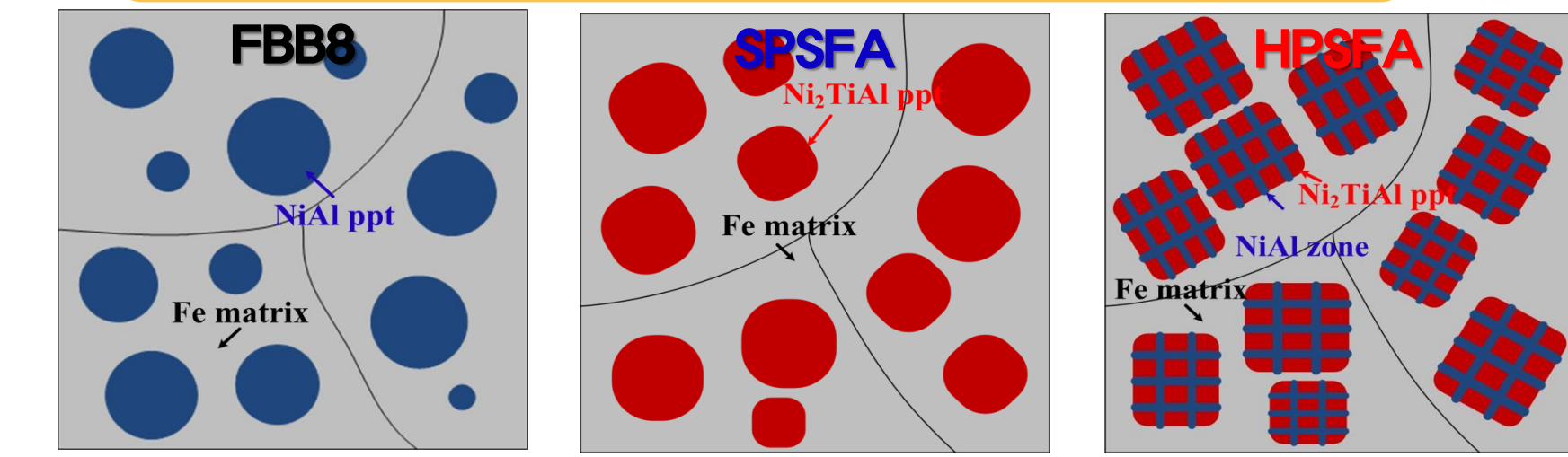
Introduction: NiAl-Strengthened Ferritic Alloys



TEM dark field image of FBB8 along [100] zone axis using <100> superlattice reflection

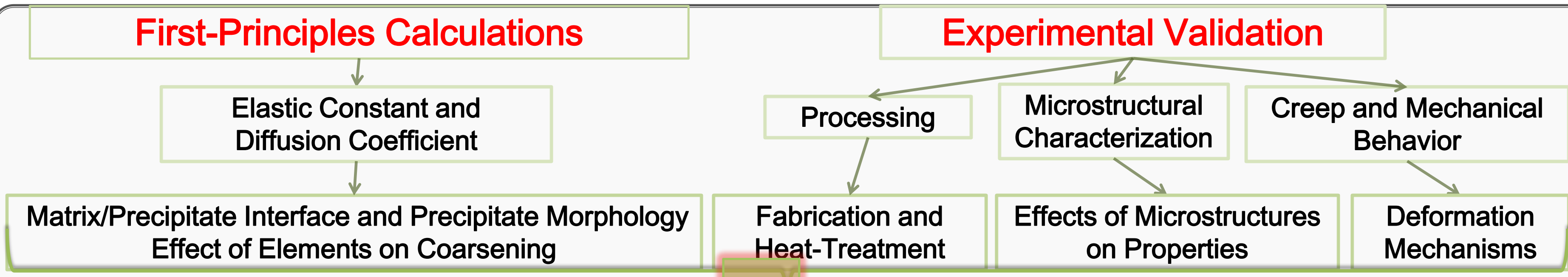
A comparison of Larson-Miller parameter plots between FBB8 and other Fe-based materials candidates for steam turbine applications.

Objective



- Introduction of new types of precipitates, (single Ni₂TiAl precipitate-strengthened ferritic alloy [SPSFA], hierarchical Ni₂TiAl/NiAl precipitate-strengthened ferritic alloy [HPSFA]).
- Understanding of the effect of precipitate structures on the creep behavior.

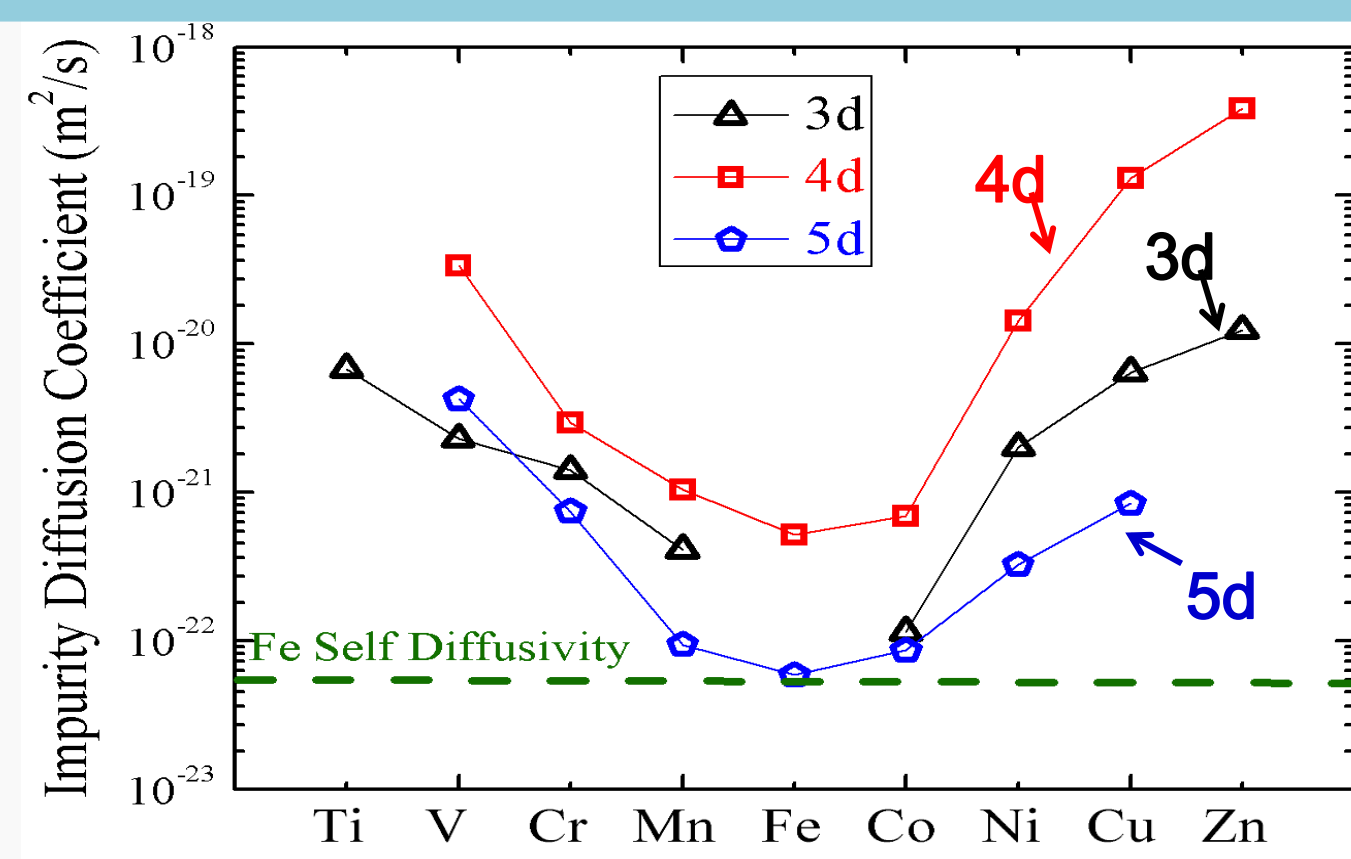
Schematic Illustration of Current Study



Optimization of creep properties of novel ferritic superalloys with a hierarchical structure

First-Principles Calculations

Harmonic Transition-State Theory Assuming Vacancy Mechanism



$$D_A^B = D_{0A}^B \exp\left[-\frac{Q_A^B}{k_B T}\right]$$

ν^* : attempt frequency for the hop of a solute atom to a nearest-neighbor vacancy

Self Diffusion in a-Fe

$$D_{0Fe}^{Fe} = a^2 f_{bcc} \exp\left[\frac{\Delta S_v^f}{k_B}\right] \times \left[\frac{\prod_{i=1}^{3N-3} v_i^{vac}}{\prod_{i=1}^{3N-4} v_i^{sad}}\right]$$

Impurity Diffusion

$$D_{0Fe}^I = a^2 f_{Fe}^I \exp\left[\frac{\Delta S_v^f + \Delta S_v^{bind}}{k_B}\right] \times \left[\frac{\prod_{i=1}^{3N-3} v_i^{vac}}{\prod_{i=1}^{3N-4} v_i^{sad}}\right]$$

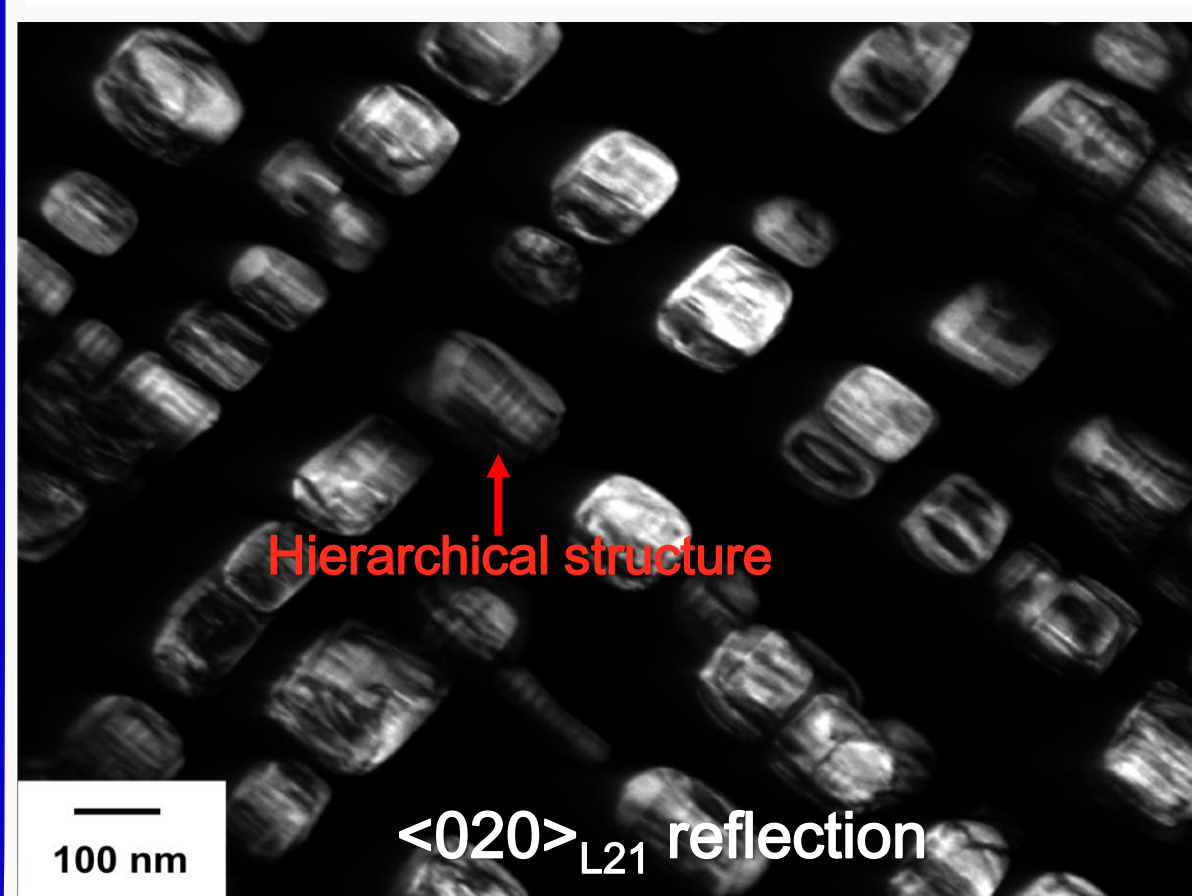
$$Q_{Fe}^I = \Delta H_v^f + \Delta H_v^{bind} + \Delta H_v^{mig,I}$$

D_0^I : pre-exponential factor
 Q_A^I : activation energy
 a : lattice constant
 f_c : correlation factor

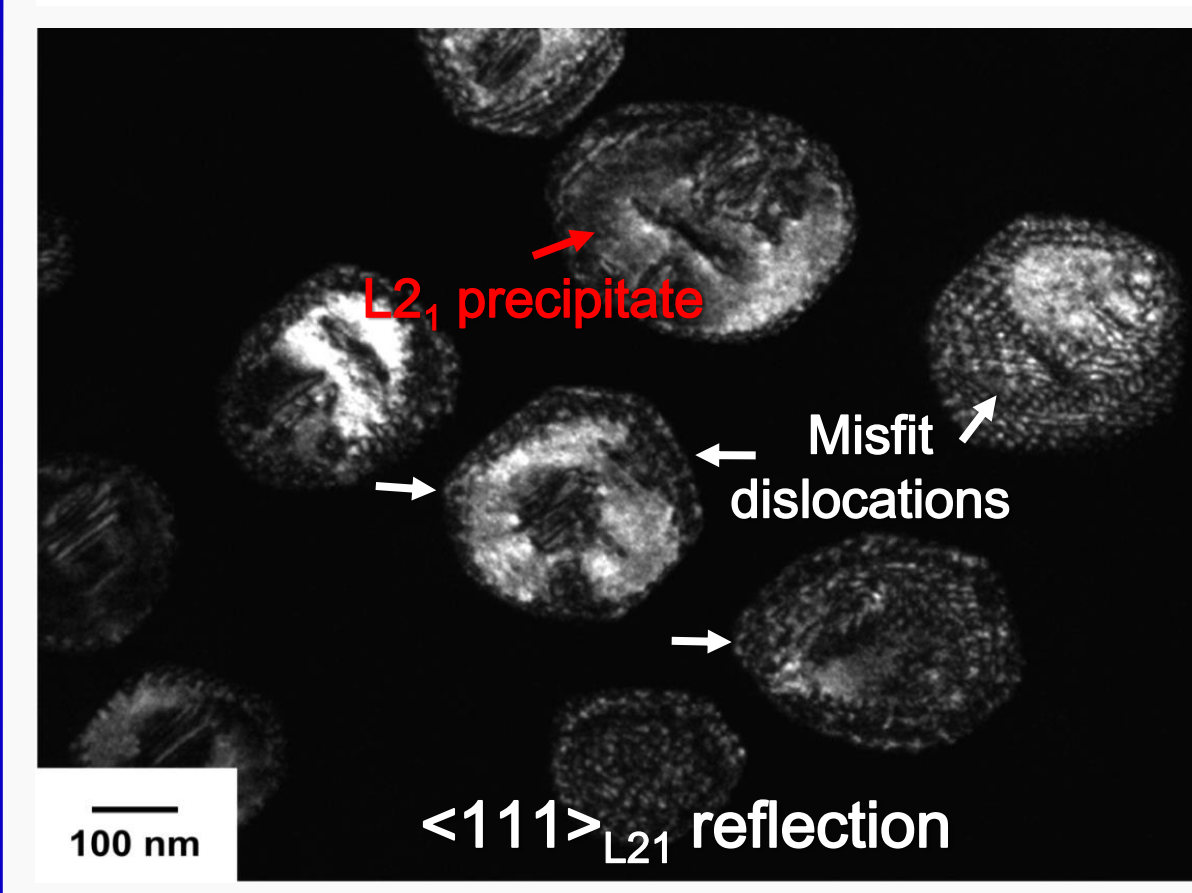
Experimental Results

Dark-Field Transmission-Electron Micrograph

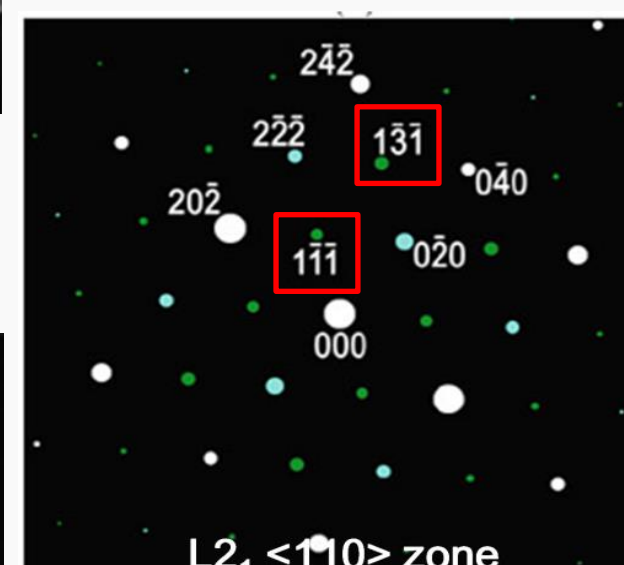
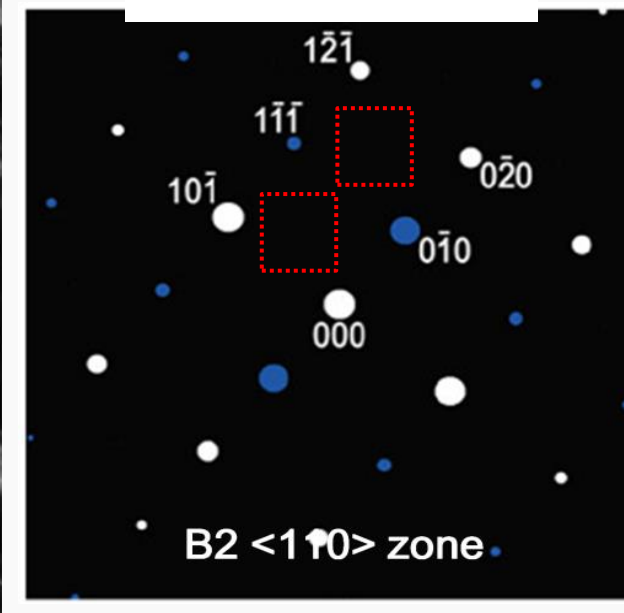
Fe-2Ti-6.5Al-10Cr-10Ni-3.4Mo-0.25Zr-0.005B (wt. %)



Fe-4Ti-6.5Al-10Cr-10Ni-3.4Mo-0.25Zr-0.005B (wt. %)



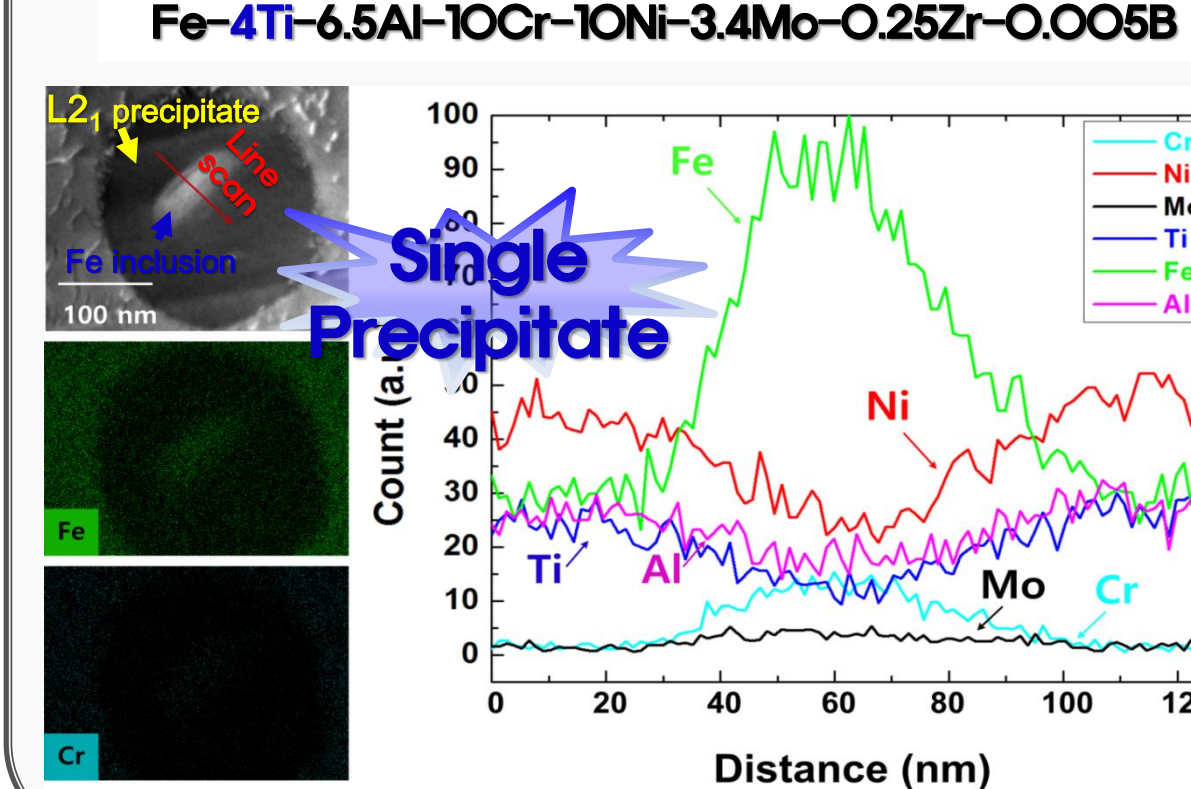
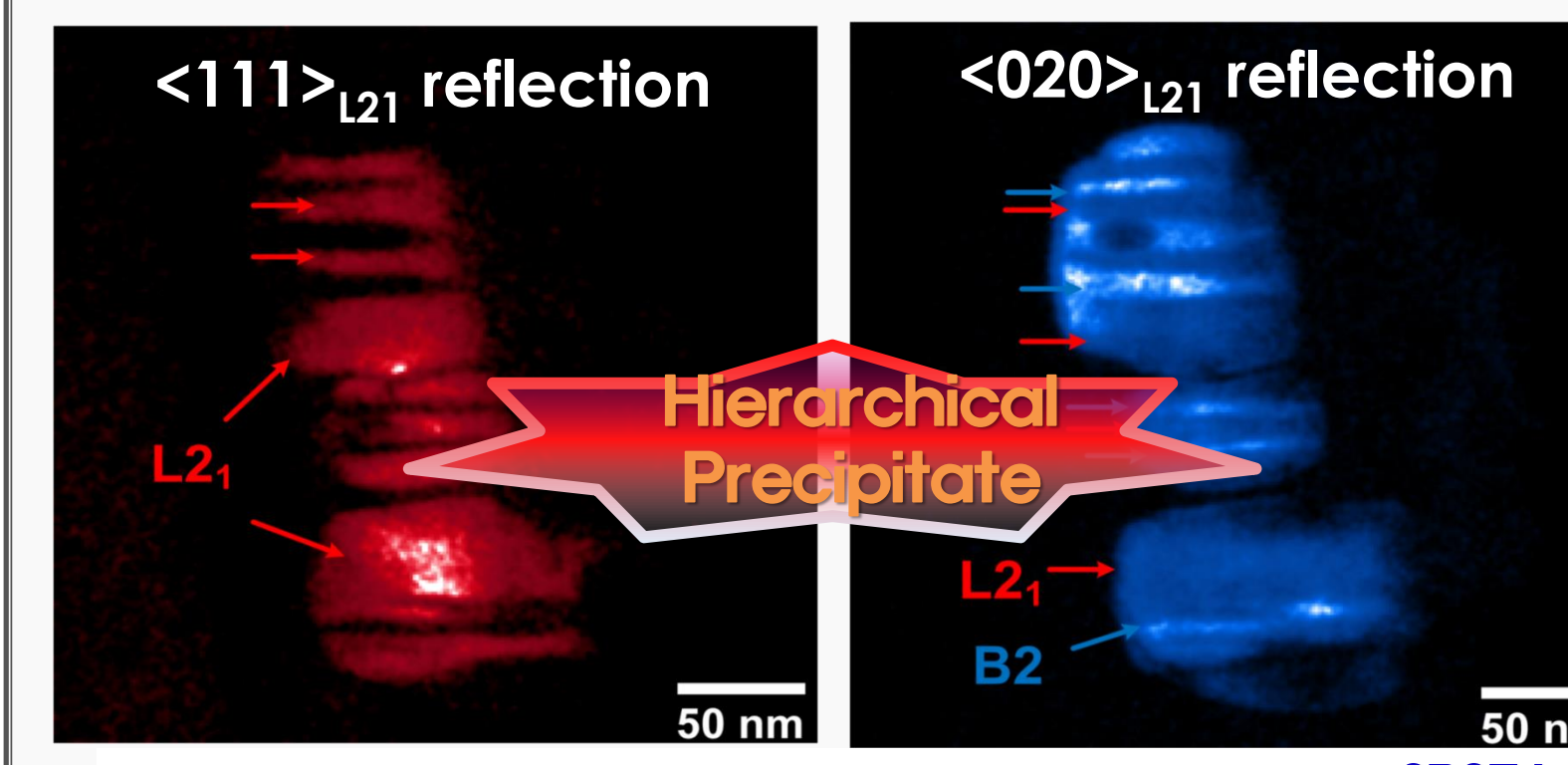
Simulated Patterns



- 2%-Ti alloy Cuboidal and coherent precipitates
- 4%-Ti alloy Spherical and semi-coherent precipitates

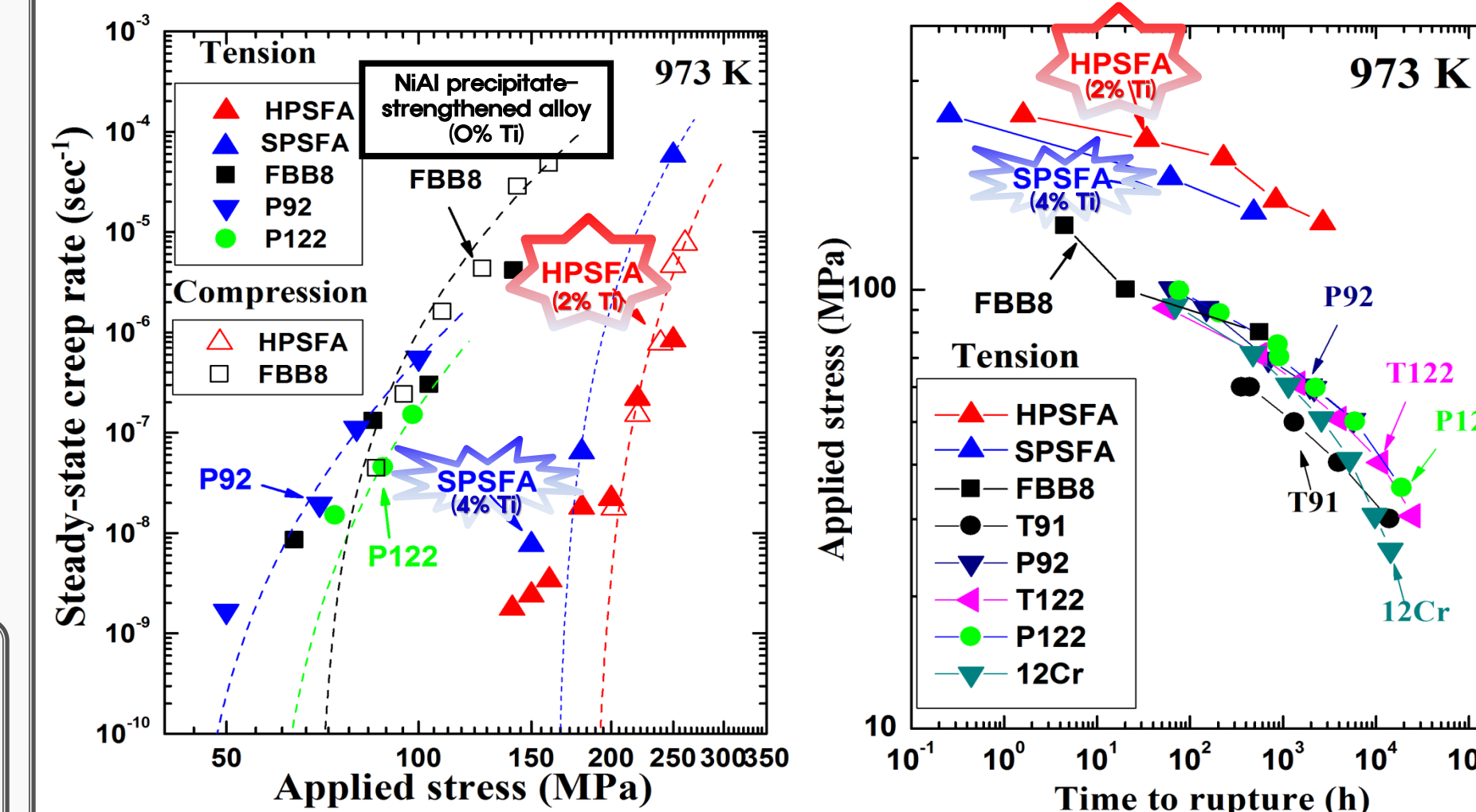
Experimental Results

Fe-2Ti-6.5Al-10Cr-10Ni-3.4Mo-0.25Zr-0.005B (wt. %) → HPSFA



- 2%-Ti alloy Hierarchical precipitate structure consisting of B2-NiAl and L2₁-Ni₂TiAl phases → HPSFA
- 4%-Ti alloy Single-phase L2₁-Ni₂TiAl precipitate structure → SPSFA

Creep Properties

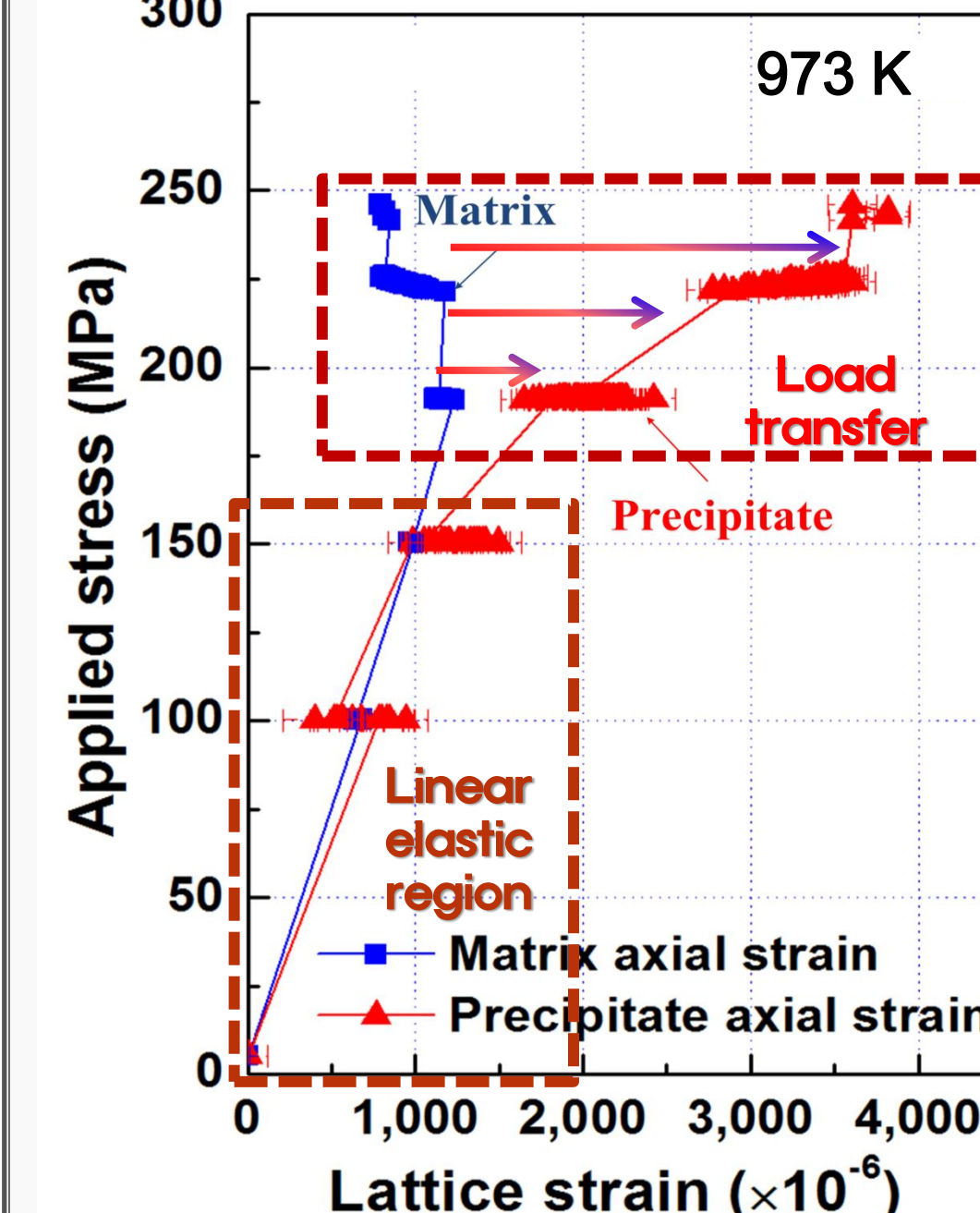


- HPSFA and SPSFA → Superior creep resistance to FBB8 and other ferritic steels
- HPSFA → Strain rates are more than four orders of magnitude lower than FBB8.
- HPSFA is much better creep resistant than SPSFA → Indication of effective strengthening of Ni₂TiAl phase and hierarchical precipitate structures, as compared to that of the single NiAl precipitate.

In-Situ Neutron-Diffraction Creep Results

Fe-6.5Al-10Cr-10Ni-3.4Mo-2.0Ti-0.25Zr-0.005B (wt. %), HPSFA

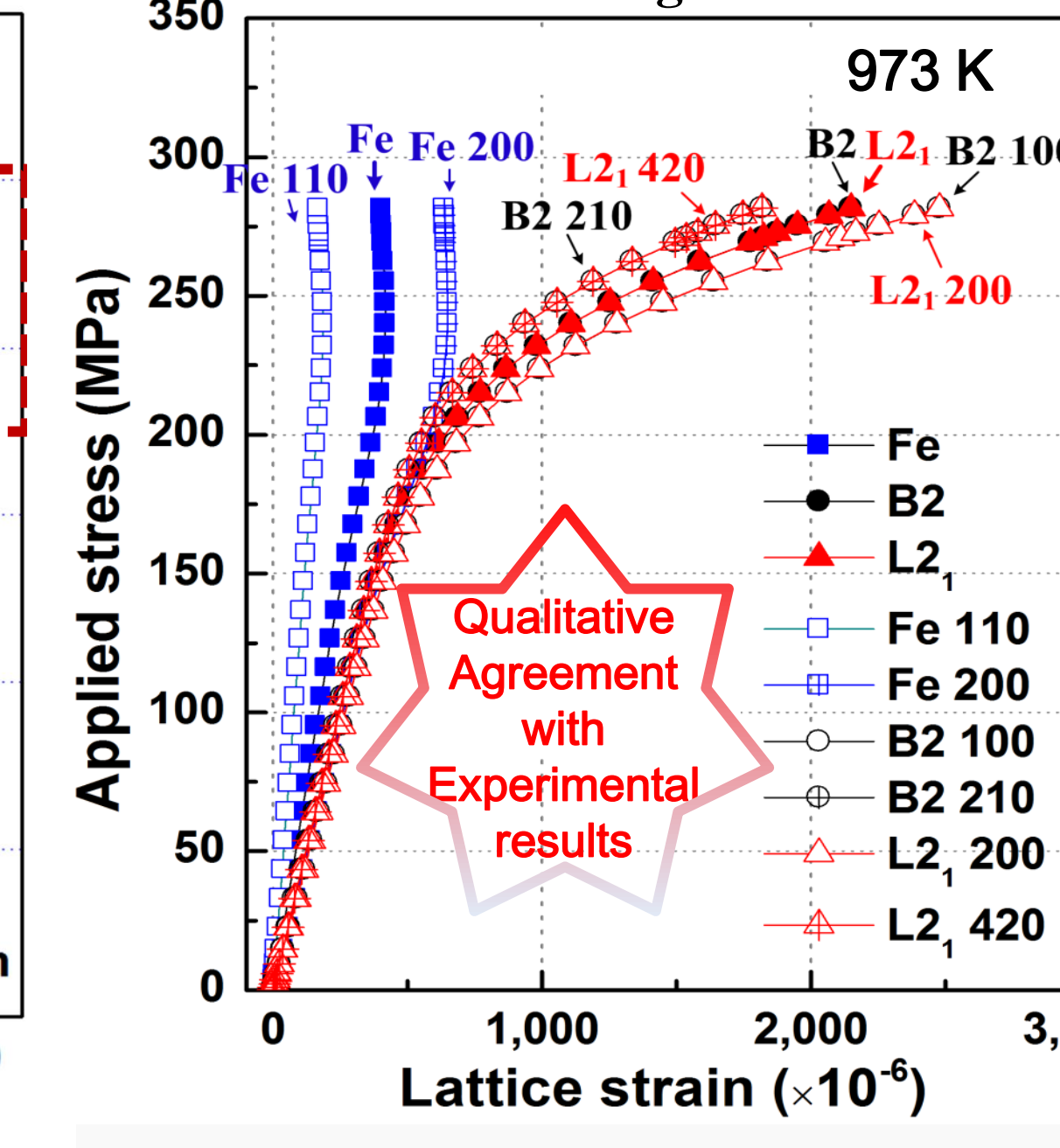
In-Situ Neutron Diffraction Experiment



$$(\text{Lattice strain}) \varepsilon = \frac{a - a_0}{a_0}$$

a = lattice parameter under loading
 a_0 = lattice parameter without loading

Crystal-Plasticity Finite-Element-Modeling Results



- A clear load-transfer from the matrix to precipitate during loading and creep at 973 K. → Indication of insufficient diffusional flow at the matrix/precipitate interface.

Future Works

1. Effects of aging temperatures and time on the hierarchical-precipitate structure and creep behavior of the 2% Ti alloy (coarsening behavior and optimization of the creep properties)
2. Systematic study of hierarchical-precipitate-strengthened ferritic alloys by substituting Ti with Hf, Ta, and Zr (Introduction of the new hierarchical-precipitate structure and its effect on the creep mechanisms)
3. Systematic creep experiments at various temperatures and stresses on the new hierarchical-precipitate-strengthened ferritic alloys (study of creep behavior and mechanisms)
4. Calculations of single-crystal elastic constants (C_{ij}) for L2₁-Ni₂HfAl, L2₁-Ni₂TaAl, and L2₁-Ni₂ZrAl from first principles (morphology of precipitates and load-partitioning condition in creep studies)
5. Calculations of interfacial energies for BCC-Fe/L2₁-Ni₂HfAl (or L2₁-Ni₂TaAl, L2₁-Ni₂ZrAl) from first principles (nucleation, coarsening resistance, and morphology of precipitates)
6. Dislocation-dynamic simulations to calculate the yield strength at room-temperature and creep-flow strength at high temperatures with various microstructures (controlling alloy microstructures to optimize the creep resistance)

Summary

1. Impurity-diffusion coefficients of 3d, 4d, and 5d in the BCC Fe matrix are calculated from first principles. It was found that the Impurity diffusion minimum for transition metal solutes is in middle of series (Ru and Os), with 5d < 3d < 4d.
2. TEM was conducted on 2% and 4% Ti alloys. It was found that the 2% Ti alloy contains a NiAl/Ni₂TiAl hierarchical precipitate, while the 4% Ti alloy consists of a single Ni₂TiAl precipitate.
3. These alloys are superior creep resistant at 973 K, as compared to the FBB8 and conventional ferritic steels. In particular, the creep rate of the 2% Ti alloy with the hierarchical precipitates is four orders of magnitude lower than FBB8.
4. From the in-situ neutron-diffraction experiments, a clear load transfer from the matrix to precipitate was observed during loading and creep deformation, which indicates the insignificant diffusional flow at the interface.
5. A crystal-plasticity finite-element model (CPFEM) shows reasonably good agreement with neutron-diffraction measurements.

Publications

1. Huang, S., Gao, Y., An, K., Zheng, L., Wu, W., Teng, Z. & Liaw, P. K. Acta Mater. 83, 137-148, (2015).
2. Liebscher, C. H., Radmilović, V. R., Dahmen, U., Vo, N. Q., Dunand, D. C., Asta, M. & Ghosh, G. Acta Mater. 92, 220-232, (2015).
3. Vo, N. Q., Liebscher, C. H., Rawlings, M. J., Asta, M. & Dunand, D. C. Acta Mater. 71, 89-99 (2014).
4. Teng, Z. K., Ghosh, G., Miller, M. K., Huang, S., Clausen, B., Brown, D. W., Liaw, P. K. Acta Mater. 60, 5362-5369, (2012).
5. Huang, S., Worthington, D. L., Asta, M., Ozolins, V., Ghosh, G. & Liaw, P. K. Acta Mater. 58, 1982-1993, (2010).

Acknowledgements

The research is supported by the Department of Energy (DOE), Office of Fossil Energy Program, under Grants of DE-09NT0008089, DE-FE0005868, DE-FE-0011194, and DE-FE-0024054 with Mr. Richard Dunst, Mr. Vito Cedro, Dr. Patricia Rawls, Mr. Steven Markovich, and Dr. Jessica Mullen as the program managers. The work has been benefited from the use of the Lujan Neutron Scattering Center at the Los Alamos Neutron Science Center (LANSCE), which is funded by the Office of Basic Energy Sciences (DOE). Los Alamos National Laboratory is operated by the Los Alamos National Security LLC under the DOE Contract number of DE-AC52-06NA-25396. This research was supported by the Center for Nanophase Materials Sciences (CNMS) at the Oak Ridge National Laboratory (ORNL), which is sponsored by the Scientific User Facilities Division, Office of Basic Energy Sciences, U.S. Department of Energy.